

Dalton Transactions

An international journal of inorganic chemistry

Accepted Manuscript

This article can be cited before page numbers have been issued, to do this please use: A. Sarkar, R. Kumar, B. Das, P. S. Ray and P. Gupta, *Dalton Trans.*, 2020, DOI: 10.1039/C9DT04720D.



This is an Accepted Manuscript, which has been through the Royal Society of Chemistry peer review process and has been accepted for publication.

Accepted Manuscripts are published online shortly after acceptance, before technical editing, formatting and proof reading. Using this free service, authors can make their results available to the community, in citable form, before we publish the edited article. We will replace this Accepted Manuscript with the edited and formatted Advance Article as soon as it is available.

You can find more information about Accepted Manuscripts in the [Information for Authors](#).

Please note that technical editing may introduce minor changes to the text and/or graphics, which may alter content. The journal's standard [Terms & Conditions](#) and the [Ethical guidelines](#) still apply. In no event shall the Royal Society of Chemistry be held responsible for any errors or omissions in this Accepted Manuscript or any consequences arising from the use of any information it contains.

Cyclometalated Trinuclear Ir(III)/Pt(II) Complex as a Luminescent probe for Histidine-rich Proteins

View Article Online
DOI: 10.1039/C9DT04720D

Received 00th January 20xx,
Accepted 00th January 20xx

DOI: 10.1039/x0xx00000x

Ankita Sarkar,^{a†} Ravi Kumar,^{b‡} Bishnu Das,^a Partho Sarothi Ray,^{*b} Parna Gupta^{*a}

Organometallic complexes have important application in the field of protein staining, with the potential for use in proteomic analysis. The rational synthesis of a trinuclear luminescent organometallic complex with two platinum(II) centres appended to the cyclometalated ligand of the iridium(III) centre is reported here. Two di-2-picolyamine groups bonded to the cyclometalated phenyl pyridine moiety provide three coordinating sites to each platinum centre. The replacement of chloride from the fourth coordination site of two square planar platinum metal centres with imidazole nitrogen or sulphur atom of histidine/cysteine is evident from the change in luminescence intensity upon binding these amino acids. The increase in luminescent emission intensity on binding of histidine to the organometallic complex allowed it to be used as a protein staining agent. Reversibility of the staining upon washing with imidazole enhances the possibility of its application in mass spectrometric analysis.

Introduction

Light-emitting materials with tunable luminescence properties are of interest due to their wide-ranging applications as chemical sensors, biological labels, organic optoelectronics and phosphorescent organic light-emitting diodes (PhOLEDs).¹ Phosphorescent organometallic complexes, including iridium, ruthenium, rhenium, copper and platinum, have especially been of interest in applications in the above areas. Besides these, another important application of phosphorescent organometallic complexes is in protein staining, a necessary procedure in proteomic studies.²

Proteomic analysis is widely used now, from basic biological research to clinical applications, and is becoming an important tool for diagnostics. However, the potential of organometallic complexes in the field of protein staining, has not been explored sufficiently. Apart from the classical silver nitrate (silver staining) and Coomassie Brilliant Blue (CBB) staining methods, SYPRO[®]Ruby, RuBPS and ASCQ Ru are the only organometallic complexes used as commercial products in protein staining.^{2h-j} The major requisites for the development of protein staining agents are compatibility with mass spectroscopic analysis, ease of staining and destaining procedures which is dependent on the nature of binding between the staining agent and the protein, and low detection limits. Silver staining is incompatible with mass spectrometry and provides unreliable quantitative results and the detection limit is only upto microgram level in case of CBB staining. The chemical composition of the widely used SYPRO[®]Ruby is patent-protected, which hinders the application of the complex universally or optimization for varied applications.^{2h} Therefore, in recent years multiple

efforts have been put to develop novel organometallic complexes as protein staining agents.

One of the approaches for staining proteins, both in gel and in cells, is to use staining agents which can specifically bind to amino acids, the constituent of proteins. Histidine is a particularly attractive amino acid for such applications, as the presence of a side chain imidazole ring allows interaction with a number of chemical groups. Histidine is also important biologically, being an essential amino acid and a neurotransmitter, and is also the precursor for histamine which is involved in many physiological processes. Also, abnormal levels of histidine-rich proteins are found in a variety of disease conditions such as liver cirrhosis and asthma. Therefore, the detection of histidine-rich proteins also has important diagnostic applications. A number of organometallic compounds have therefore been developed to selectively stain histidine or histidine-rich proteins. For example Wong et al. and Li et al. reported the synthesis of non-emissive Ir(III) complexes which could selectively bind to histidine-rich proteins based on a luminescent switch-on mechanism through replacement of coordination ligands.^{2g} However, the problem with this type of staining agents is that they would covalently bind with histidine residues in proteins, making them incompatible with downstream mass spectrometric analysis. Therefore, there is a need to develop protein staining agents which can reversibly bind to proteins, and preferably in which the luminescence and protein binding are dependent on different functional groups. This will allow tunability of the luminescence property, without affecting protein binding, and allow for more versatile applications of such compounds.

The application of cyclometalated heteroleptic iridium(III)/platinum(II) complexes of polypyridyl ligands as protein staining agents both in gels and in cells provide a number of important advantages which include chemical and photochemical stability, permeability, minimization of self-quenching due to the significant Stokes' shift, long-lived triplet excited state ($\tau \sim \mu\text{s}$) that help to eliminate the short-lived autofluorescence of biological samples.³ The iridium(III) complexes particularly exhibit a high luminescent quantum yield in organic solvent and moderate in aqueous solutions. Recently, platinum(II) complexes with bidentate ligands have also been reported as protein staining agents both in gels

^a Department of Chemical Sciences,

^b Department of Biological Sciences

^c contributed equally

Indian Institute of Science Education and Research-Kolkata, Mohanpur, West Bengal 741246, India

^d E-mail: parna@iiserkol.ac.in; E-mail: psray@iiserkol.ac.in:

Fax: +91 3473279131; Tel: +91 3473279130 Electronic Supplementary Information (ESI) available: [details of any supplementary information available should be included here]. See DOI: 10.1039/x0xx00000x

e.

and in live cell imaging.^{2a,b} A previous report in the literature has demonstrated a heterobimetallic Ru(II)/Pt(II) complex as a sensor selective for sulfhydryl-containing amino acids and peptides.^{2j} However no such compounds have been reported for binding to histidine or histidine-rich proteins. Rationally designed heterobimetallic complexes may provide different centres for reversible amino acid binding and fluorescent emission. Therefore, we have endeavoured to develop a heterobimetallic complex containing Ir(III) and Pt(II) as a specific sensor for histidine and a staining agent for histidine-rich proteins.

The rational designing of a trinuclear organometallic complex **3**, with two Pt and one Ir centres is reported here. The Pt centres are coordinated to dipicolylamine unit from three sites and the fourth coordination site is occupied by a chloride ion. These two Pt centres are connected individually to the cyclometalating ligand coordinated to Ir(III) centre. The histidine residues from proteins reversibly coordinates with the Pt centre replacing the chloride ion with the increase in the emission intensity. This complex showed efficient binding to histidine in solution and ability to reversibly stain hexa-histidine-tagged and untagged proteins in gels with differential sensitivity, demonstrating a potential for application as a protein staining agent.

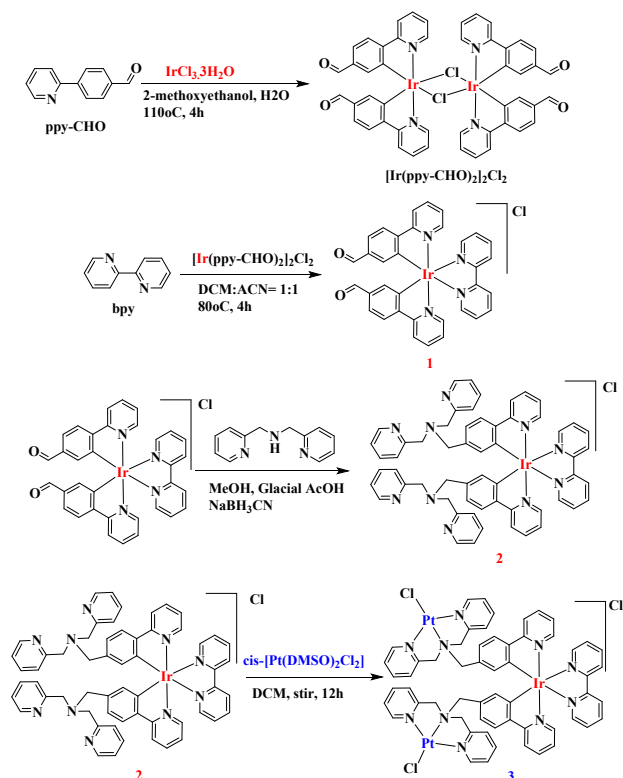
Result and Discussion

Synthesis and analytical characterization

The stepwise synthesis of heterotrinnuclear complex **3** starts with the synthesis and purification of mononuclear previously reported iridium complex **1** as shown in **scheme 1**.⁴ In a typical method $[\text{Ir}(\text{ppy-CHO})_2\text{Cl}]_2$ was dissolved in dichloromethane(DCM):acetonitrile(ACN)(1:1) and heated for a while, followed by the addition of 2,2'-bipyridyl and the resulting solution is refluxed for another 4h. Complex **1** was purified by TLC with 5% methanol(MeOH) in DCM. The purity of the complex has been checked by ¹H NMR. The intermediate mononuclear iridium complex **2** was synthesized with the reaction of di-2-picoylamine with **1** in the presence of catalytic amount of glacial acetic acid followed by sodium cyanoborohydride in methanol. The treatment with saturated sodium carbonate solution and washing of the organic layer several times with water afford complex **2**. The pure complex **3** separates out of the solution when complex **2** is stirred with $[\text{Pt}(\text{dmsO})_2\text{Cl}_2]$ in dichloromethane for 8h. The formation of complex **2** and trinuclear complex **3** were initially checked with ESI-MS spectra and ¹H,¹³C NMR and elemental analysis confirmed the purity (**Figure S1, S2**). Good quality crystal could not be obtained, however, geometry optimized structures (**Figure 1**) provided the information about the disposition of the 2-picolylamine moiety as well as trinuclear Pt-Ir-Pt (**3**) molecular orientation.

Photophysical study

Absorption spectra of all the three complexes were recorded in degassed methanol (**Figure 2**). The spectra of the



Scheme 1: Stepwise synthesis of complexes **1-3** starting from iridium(III) and platinum(II) precursors

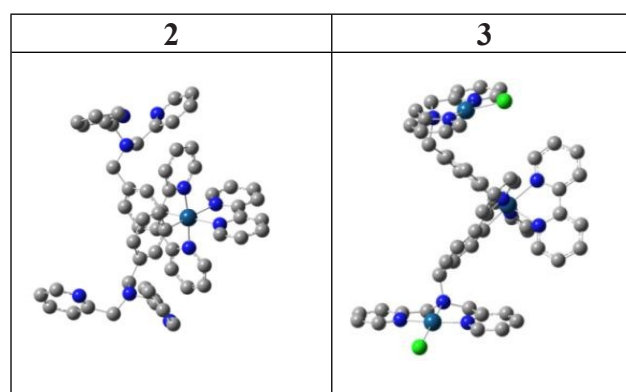


Figure 1: Geometry optimized structure of complexes **2** and **3** (hydrogen atoms are omitted for clarity)

cyclometalated iridium (III) complexes usually witness metal to-ligand charge transfer (MLCT) and ligand centered (LC) transitions. Intense high energy bands around 300 nm with $\epsilon \approx 0.5 - 3 \times 10^5 \text{ M}^{-1}\text{cm}^{-1}$, assigned to spin allowed ligand-centered¹IL transitions ($1\pi \rightarrow \pi^*$) from both the ppy-CHO (cyclometalated ligand, **Scheme 1**) to bpy(2,2'-bipyridine) ligands for **1** and ppy-dpa (di-2-picolylamine appended phenylpyridine) \rightarrow bpy for **2** and **3**.⁵ The absorption shoulders between 340 - 410 nm with moderate extinction coefficients have been assigned to an admixture of spin-

A. allowed metal-to-ligand charge transfer ($^1\text{MLCT}$), $d\pi - \pi^*$ (bpy) and ligand-to-ligand charge transfer ($^1\text{LLCT}$), $\pi(\text{bpy}) - \pi^*(\text{bpy})$ processes (**Table 1**).⁵ The low intensity band ($\epsilon \approx 2-3 \times 10^3 \text{ M}^{-1}\text{cm}^{-1}$) around 450 nm (shoulder) for 1 and 480 nm for 2 and 3 are due to the spin-forbidden transitions owing to $^3\text{MLCT}$ and $^3\text{LLCT}/^3\text{LC}$ transitions. Mostly $\pi(\text{ppy-dpa}$ of 2, 3), metal orbital to $\pi^*(\text{bpy})$ are involved in the transition as evident from the theoretical calculations (**Table S1**). The optimization of the geometry and TDDFT studies have been done by using the spin-unrestricted UB3LYP approach.⁶

The emission spectra of the complexes 1, 2 and 3 were recorded in methanol at 273K and 77K (**Figure 2**). The emission of 1, 2 and 3 show broad spectrum with maxima at 562, 578 and 552 nm ($\lambda_{\text{ex}} = 400 \text{ nm}$, $\lambda_{\text{em}} = 460 \text{ nm}$ is due to Raman Scattering) respectively. The emission lifetime of all the three complexes (**Figure 2**) confirm the phosphorescence nature of the emission. To understand the nature of transition of the PL(photoluminescence) spectra were recorded in frozen methanol-2MeTHF (77K). Complexes 1 and 2 show large red-shifted λ_{max} at 673 nm and 661 nm, whereas, complex 3 emits at 589 nm. To understand about the nature of transition we record the PL spectra of neat(solid) film (**Figure 2**) and interestingly rich vibronic structures in the emission band was observed for complexes 1 and 2. Analysis of the emission spectra of complexes 1 and 2 in solid film at 77K suggest the emission at 562 nm and 578 nm at 273 K are basically contributed by two different emission at 545, 590 nm for 1 and 554, 605 nm for 2 assigned to $^3\text{MLCT}$ and $^3\text{LLCT}$.⁷ The nature of broad emission band for complex 3 remain unchanged. Thus, the emission is attributed to $^3\text{MLCT}$ only.

Amino-acid sensing

The complex 3 is moderately emissive in 50 μM PBS buffer solution and luminescence sensing of amino acids⁸ was recorded in the same buffer solution. Initially, individual amino acids were titrated against complex 3, as shown in

Figure 3. The emission intensity ($\lambda_{\text{ex}} = 400\text{nm}$) decreases (4.3 fold) with the addition of cysteine (Cys, 100 μM) to complex 3 (10 μM). Separately, a ~ 5.0 fold increase in emission intensity is observed with addition of histidine (His, 100 μM). The luminescence response of complex 3 to other amino acid shows that the emission intensity remains practically unchanged. So, it can be concluded that luminescence enhancement occurs only in presence of histidine. The emission intensity reaches saturation level at $[\text{His}]/[\text{Ir}]$ 2.5: 1 (**Figure S4**). It is evident from the literature that platinum(II) binds to histidine and cysteine through imidazole nitrogen⁹ and sulphur atom.¹⁰ Platinum has greater propensity to interact with soft sulphur and borderline imidazole over chloride moiety. The emission spectra with Boc-protected L-histidine as well as L-histidinemethylester were also recorded. The increase in emission intensity supports that it is the imidazolyl nitrogen that interact with platinum centre (**Figure S3**). Methionine was also expected to coordinate the platinum centre in the same manner as cysteine (through sulphur), however the methyl group in methionine sterically hinders the approach of the sulphur to bind to the platinum centre. To understand the competitive behaviour between histidine and cysteine, we did the titration of complex 3(10 μM) + histidine ($5 \times 10^{-5}\text{M}$) with increasing amount of cysteine and vice-versa (**Figure S5**). It is observed that, with addition of histidine (10 μM) to 3 + cysteine ($5 \times 10^{-5} \text{ M}$), emission intensity increases two-fold and becomes maximum after addition of histidine (final histidine conc: 80 μM). Whereas, addition of cysteine to the combined solution of 3 and histidine does not show any effect (**Figure S4**). This observation indicates that, though platinum-cysteine-S bond is more favourable for their soft-soft interaction, the highly labile nature of Pt-S bond can easily be replaced by imidazole upon addition of histidine.¹¹

Table 1: Photophysical parameters for the complexes 1 – 3

Complex	$\lambda_{\text{abs}}^{\text{a}}$ (nm) (b)	273K			77K			
		$\lambda_{\text{em}}^{\text{a,c}}$ (nm)	τ^{a} (μs)	ϕ^{d}	$\lambda_{\text{em}}^{\text{a,c}}$ (nm)	τ^{a} (μs)	$\lambda_{\text{em}}^{\text{c,f}}$ (nm)	τ^{f} (μs)
1	450e(0.158), 424(0.208), 363(0.338), 297(2.009), 269(2.390)	562	5.8	3.5	673	9.8	545, 590, 634, 656	9.0
2	477(0.039), 410(0.194), 379(0.350), 344(0.523), 310(1.239), 260(2.969)	578	6.7	10.2	661	9.0	554, 605, 655	11.3
3	478(0.0226), 412(0.0904), 340(0.223), 292(0.765), 260(0.998)	552	7.1	4.9	589	17.1	586	5.0

^a Methanol. ^b $\epsilon \times 10^{-4} \text{ M}^{-1} \text{ cm}^{-1}$. ^c $\lambda_{\text{ex}} = 400\text{nm}$. ^d The quantum yield in degassed methanol solution was estimated relative to $[\text{Ru}(\text{bpy})_3](\text{PF}_6)_2$ in acetonitrile as the standard ($\phi_{\text{em}} = 5.9\%$). ^e Shoulder. ^f solid film.

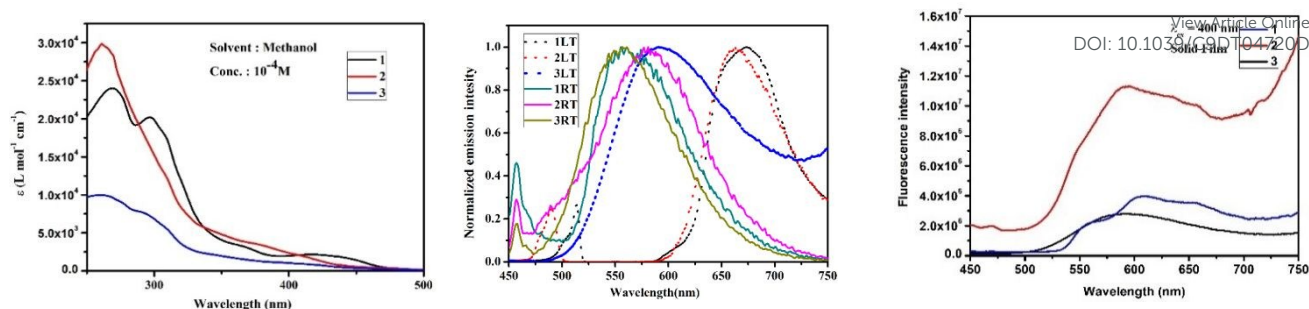


Figure 2: A) Electronic absorption spectra of 1- 3 (degassed methanol) B) Normalized Emission spectra ($\lambda_{ex} = 400\text{nm}$) in degassed MeOH (298K: RT, $1 \times 10^{-5}\text{M}$, solid line), and frozen solution (77K: LT, methanol, 2Me-THF, dotted line) C) Emission with solid film on glass.

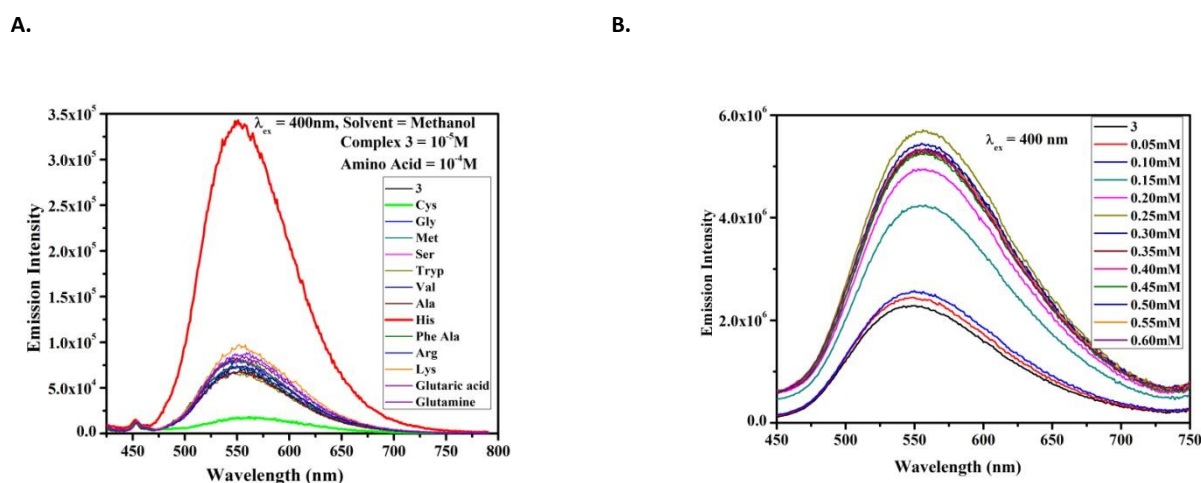


Figure 3: Emission spectra of complex 3 in presence of several L-amino acids in 50 μM PBS buffer solution (A) Complex 3 (10 μM), L-amino acid (100 μM) (B) 3 (10 μM) + histidine (starting from $5 \times 10^{-5}\text{M}$)

Protein binding and emission

As complex 3 showed a strong enhancement in PL intensity on specific interaction with histidine, we investigated whether it showed enhanced emission intensity on interaction with histidine-containing proteins. Phosphorescence emission at 535 nm was measured on interaction of a fixed concentration of hexa-histidine-tagged, bacterially expressed and purified protein with increasing concentrations of complex 3. There was a linear increase in emission intensity on increasing concentrations of complex 3, which went upto 6×10^3 fold (Figure 4A). Complex 3 also showed a concentration-dependent enhancement in fluorescent intensity on binding to a non-histidine tagged protein (BSA) but the enhancement was only around 1.6×10^3 fold (Figure 4B). Conversely, interaction of a fixed amount of complex 3 with increasing concentrations of the protein also showed a linear enhancement of emission (Figure 4C). The phosphorescence emission also showed a time-dependent increase on interaction between fixed concentrations of complex 3 and protein (Figure 4D). Together,

these observations demonstrated that complex 3 could specifically interact with proteins and show enhancement in phosphorescence, and the enhancement was dependent on the histidine content of the protein. In order to further check that increase in the emission intensity was specifically due to binding with the histidines in the protein, the same was measured on binding of constant amount of complex 3 with a constant amount of hexa histidine-tagged protein in presence of increasing concentrations of Ni-NTA, which can bind to the imidazole ring of histidine and should thereby inhibit the binding of complex 3 to the protein. It was observed that increasing concentrations of Ni-NTA showed a reduction in emission intensity, demonstrating that inhibition of binding to histidines in protein resulted in reduction of phosphorescence emission from complex 3 (Figure 4E). A similar reduction in emission intensity was observed when complex 3 interacted with histidine in presence of increasing concentrations of $\text{Ni}(\text{NO}_3)_2 \cdot 6\text{H}_2\text{O}$, which would inhibit histidine interaction with complex 3 (Figure 4F).

Staining of protein in gels

As complex 3 showed the ability to bind to histidine-containing proteins in solution and exhibit phosphorescence, we tested the ability of complex 3 to stain proteins resolved by SDS-polyacrylamide gel electrophoresis. Complex 3 showed the ability to stain bacterially expressed and partially purified hexahistidine-tagged protein in gel over a wide range of concentrations (2.5 – 20 μg), when proteins resolved in gel was incubated in a 10^{-5} M solution of complex 3, washed with water and imaged at 535 nm (**Figure 5A**). It also showed the ability to stain BSA, but with a lesser intensity. The staining was found to be stable as there was nearly equal intensity of staining on washing with water for 10 min or for 12 hours, and the stain was retained even after washing with water for 24 hours (**Figure 5A**). We also checked whether the staining was stable in presence of an organic protein fixing agent, and found that the stain was retained on washing with 30% methanol for 10 min and overnight (**Figure 5B**). Thereafter we checked whether the protein staining was a specific property of complex 3 and therefore compared the protein staining by complex 3 with that by its synthetic precursors, complex 1 and complex 2. Complex 3 showed much higher protein staining compared to complex 1 and 2, suggesting that the protein staining was a specific property of the heterobimetallic complex 3 (**Figure 5C**). We then compared the sensitivity of protein detection by complex 3 with that of the widely used, commercially available staining agent SYPRO RUBY. Complex 3 showed nearly similar sensitivity as SYPRO RUBY, with both being able to detect as low as 125 ng of protein, although the intensity of staining was slightly higher with Sypro Ruby (**Figure 5D**). Finally, we tested the reversibility of the staining with complex 3. Washing with a 500 mM solution of imidazole overnight removed nearly 90% of the staining with complex 3, showing that staining with complex 3 could be reversed by imidazole that inhibited the interaction with histidine (**Figure 5E**).

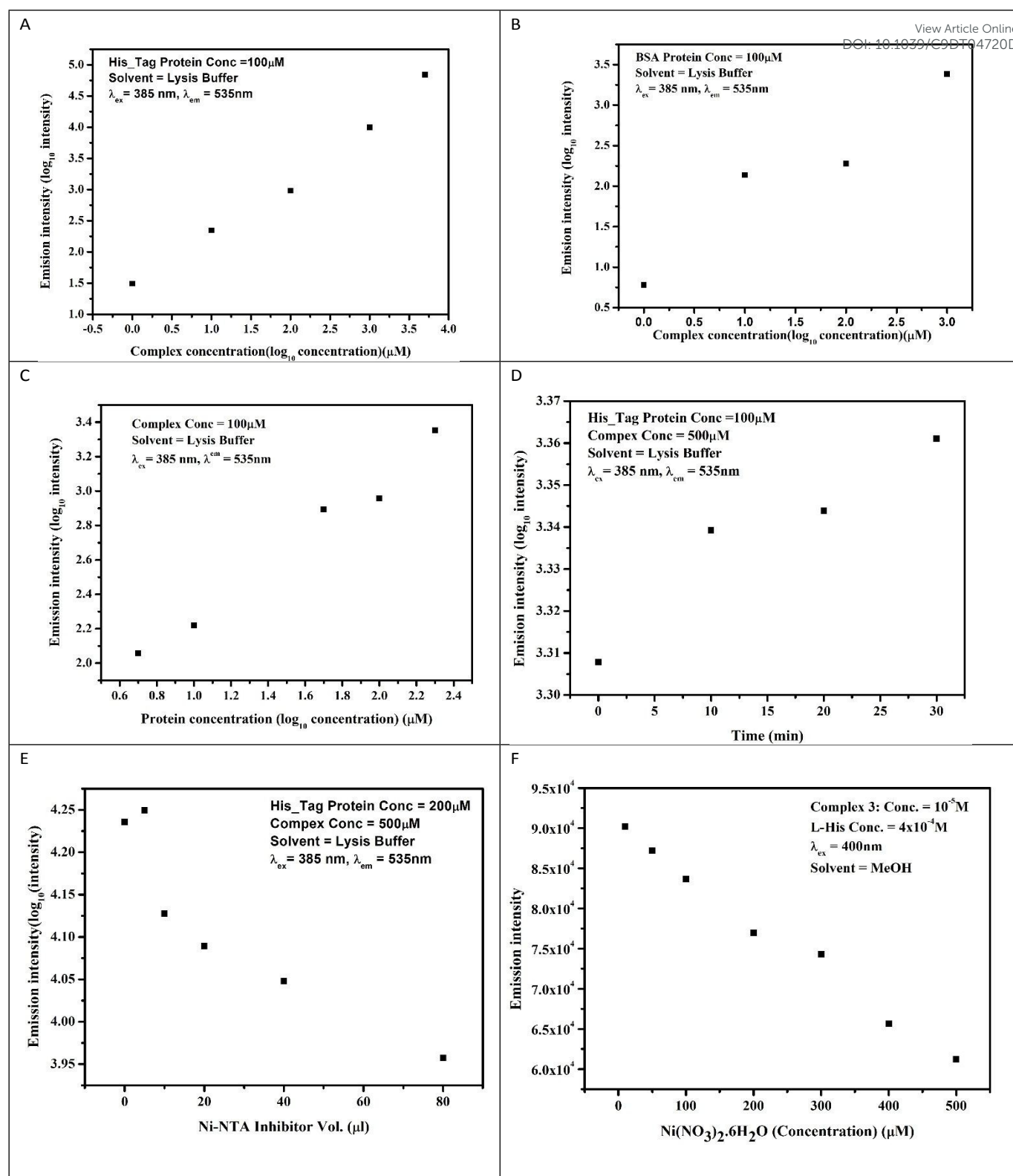


Figure 4. Protein binding and emission enhancement by complex 3. A. Phosphorescence emission at 535 nm on interaction of increasing concentrations of complex 3 (0–10 μM) with 10⁻⁴ M of bacterially expressed, purified His-tagged protein. B. Phosphorescence emission at 535 nm on interaction of increasing concentrations of complex 3 (0–10 μM) with 10⁻⁴ M of BSA. C. Phosphorescence emission at 535 nm on interaction of increasing concentrations of His-tagged protein with 10⁻⁵ M complex 3. D. Phosphorescence emission on interaction of 2 × 10⁻⁴ M His-tagged protein with 10⁻⁵ M complex 3 from 0–20 min. E. Phosphorescence emission on interaction of 10⁻⁴ M His-tagged protein with 5 × 10⁻⁴ M complex 3 in presence of increasing amounts of Ni-NTA. F. Phosphorescence emission on interaction of 4 × 10⁻⁴ M of L-histidine with 10⁻⁵ M complex 3 in presence of increasing amounts of Ni-NTA.

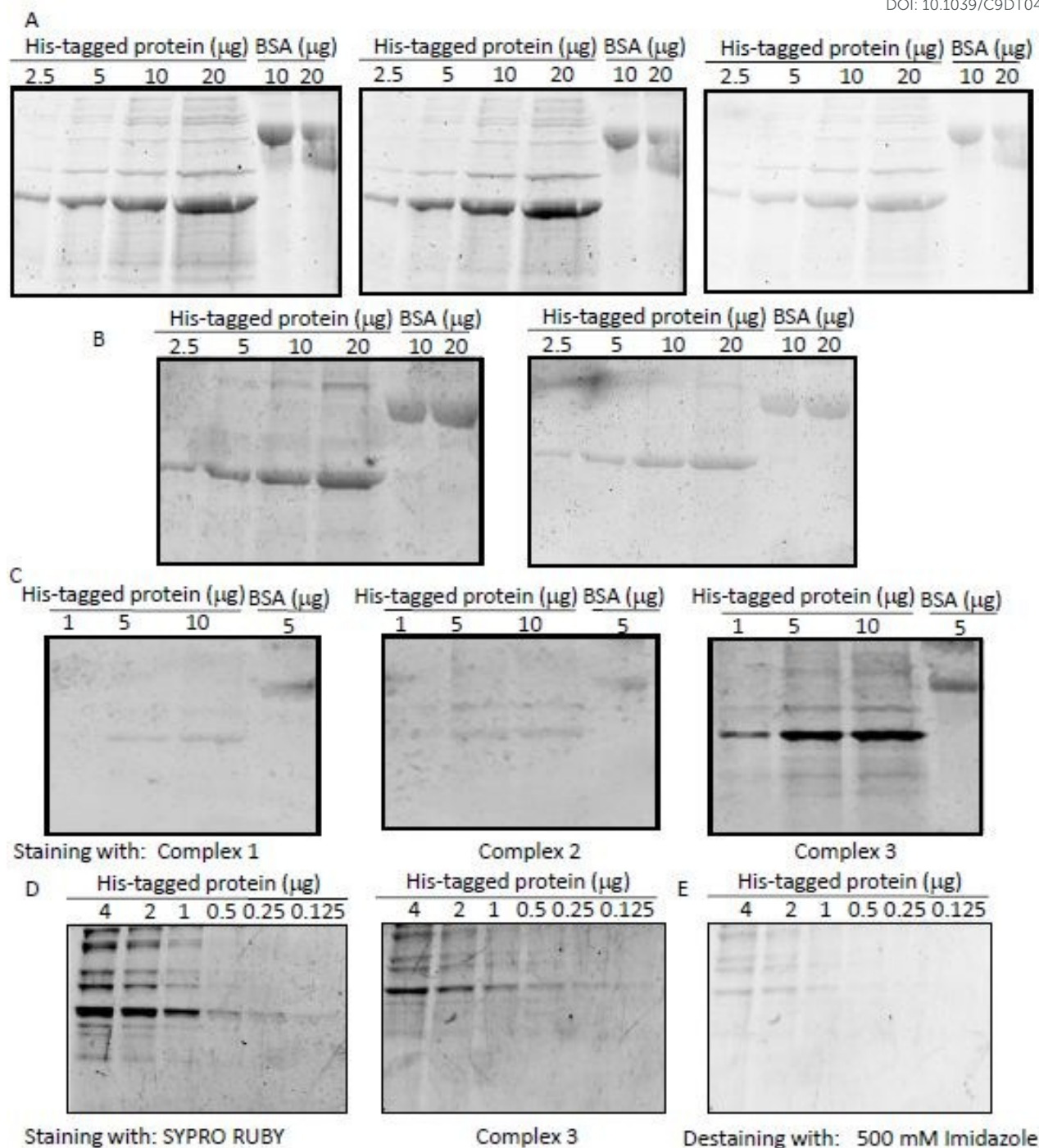


Figure 5. In-gel protein staining by complex 3. A. Staining of increasing concentrations (2.5, 5, 10 and 20 mg) of bacterially expressed, purified His-tagged protein and two increasing concentrations (10 and 20 mg) BSA with a 10^{-5} M solution of complex 3 in water. The 3 gels represent 3 washes of 10 minutes with water, 12 hour wash with water and 24 hour wash with water respectively. Phosphorescence images were taken after excitation at 488 nm. B. Staining of increasing concentrations (2.5, 5, 10 and 20 mg) of bacterially expressed, purified His-tagged protein and two increasing concentrations (10 and 20 mg) BSA with a 10^{-5} M solution of complex 3 in water. The 2 gels represent 12 hour wash and 24 hour wash with 30% methanol respectively. C. Staining of increasing concentrations (1, 5 and 10 mg) of bacterially expressed, purified His-tagged protein and one concentration (5 mg) BSA with 2×10^{-5} M solution of complex 1, 2 and 3 in respectively. The gels were fixed and washed with 30% methanol. D. Staining of decreasing concentrations (4 mg, 2 mg, 1 mg, 500 ng, 250 ng and 125 ng) of bacterially expressed, purified His-tagged protein with SYPRO RUBY (left gel) and 2×10^{-5} M solution of complex 3 in water (right gel) respectively. The gels were fixed and washed with 30% methanol. E. Staining of decreasing concentrations (4 mg, 2 mg, 1 mg, 500 ng, 250 ng and 125 ng) of bacterially expressed, purified His-tagged protein with 2×10^{-5} M solution of complex 3 in water. The gel was washed with 500 mM imidazole overnight

Experimental Section

The starting materials $\text{IrCl}_3 \cdot 3\text{H}_2\text{O}$, 4-(2-pyridyl)benzaldehyde, 2,2'-bipyridyl, di-(2-picoyl)amine and K_2PtCl_4 were purchased from Sigma-Aldrich and were used without purification.

Analytical grade solvents were obtained from commercial suppliers and dried by usual methods prior to use. Ligands were synthesized using procedures described in literature. Elemental analysis was performed with Perkin Elmer CHN Analyzer (2400 series). ^1H spectra were recorded at 25°C on a JEOL ECS 400 using TMS as the internal standard. Elemental analyses were determined on a Perkin-Elmer. Mass spectra were recorded on a Q-ToF Micromass spectrometer and Bruker mass spectrometer by positive-ion mode electrospray ionization. The electronic spectra were recorded with a U-2900 spectrophotometer from Hitachi. The emission measurements and phosphorescence lifetime were performed with a Fluoromax 3 spectrofluorometer from Horiba Jobin Yvon. Quantum yield reported here were measured relative to $\text{Ru}(\text{bpy})_3\text{Cl}_2$ in acetonitrile ($\lambda_{\text{ex}} = 450\text{nm}$, $\phi = 0.059$). The integration of the emission spectra was obtained from the Fluoromax-4 instrument from Horiba Jobin Yvon equipped with a 150W Xe lamp directly. All calculations were performed in Gaussian 09. Singlet and triplet ground state geometries were optimized using the density functional hybrid model B3LYP together with 631g(d,p) basis set and the Hay-Wadt-ECP (LANL2DZ). Frontier molecular orbitals were computed on the singlet ground state structures while the absorption transitions were assigned by TD-DFT at the same level of theory. For visualization, Gauss View was used.⁶

Synthesis

[Ir(ppy-CHO)₂]₂Cl₂: Iridium trichloride (100mg, 0.284 mmol) was refluxed for 4 hours at 110°C with 4-(2-pyridyl)benzaldehyde (104.09mg, 0.568 mmol) in 2-methoxyethanol and distilled water (3:1). Once the reaction was over and was cooled to room temperature, distilled water was poured in the reaction mixture. Orange coloured precipitate was obtained which was further washed with distilled water. The desired product after being dried in vacuum was obtained as orange solid. Yield: 98mg (98%).

Complex 1: 2,2'-bipyridyl (28mg, 0.17 mmol) was refluxed overnight at 80°C with [Ir(ppy-CHO)₂]₂Cl₂ (100mg, 0.17 mmol) in dichloromethane and acetonitrile (1:1) solution to afford a reddish- orange coloured solution. The solvent was evaporated under reduced pressure. The reddish-orange solid so obtained was redissolved in minimum amount of dichloromethane and was purified by preparative TLC with (5% methanol in dichloromethane) as second major fraction. The desired orange solution was collected and dried under reduced pressure. Yield: 77.1mg (64%).

Complex 2: Complex 1 (20mg, 0.028mmol) and di-(2-picolyl)amine (11.2mg, 0.056mmol) were dissolved in fresh methanol. A catalytic amount of glacial acetic acid was added to the solution, which was refluxed for 0.5 h. The reaction mixture was cooled by using an ice bath and then sodium cyanoborohydride (8.04mg, 0.112mmol) was slowly added to the solution. The ice bath was removed and the reaction mixture was stirred overnight at room temperature. Basic work-up was carried out using saturated aqueous sodium carbonate solution and subsequent extraction using dichloromethane was done. The organic layer was recovered, dried over anhydrous

magnesium sulphate and concentrated by vacuum. The crude product was purified by preparative TLC (5% methanol in dichloromethane, 1% ammonium hydroxide solution) as 3rd fraction. The desired yellow solution was collected and dried under reduced pressure. Yield: 11mg (30%). CHN Analysis: C₅₈H₅₀ClN₁₀Ir: Calculated: C: 62.49; H: 4.52; N: 12.56. Found: C: 62.97; H: 4.19; N: 13.01.

Exact Mass: [M] = 1114.35; [M]⁺ = 1079.38; Observed: [M]⁺ = [M]-Cl = [M]⁺ = 1079.3867;

^1H NMR (400MHz, CDCl₃) δ (ppm): 8.93 (d, 2H, $J = 8.4$), 8.43 (d, 6H, $J = 4.58$), 8.17 (t, 2H, $J = 7.63$), 7.90 (d, 2H, $J = 8.4$), 7.84 (d, 2H, $J = 4.58$), 7.79 (t, 2H, $J = 7.63$), 7.62 (d, 2H, $J = 8.4$), 7.55 (t, 4H, $J = 7.6$), 7.51 (d, 2H, $J = 5.3$), 7.24 (d, 4H, merged with nmr solvent), 7.11-7.10 (b, 6H), 7.06 (t, 2H, $J = 6.9$), 6.35 (s, 2H), 3.63 (s, 8H), 3.42 (s, 4H).

^{13}C NMR (400MHz, CDCl₃) δ (ppm): 159.76, 155.70, 150.61, 150.19, 149.22, 148.79, 142.38, 139.68, 137.13, 137.00, 132.04, 127.83, 126.46, 125.43, 123.81, 123.16, 122.86, 121.73, 119.44, 60.18, 58.54.

cis-[PtCl₂(DMSO)₂]: K₂PtCl₄ (500mg, 1.20mmol) was dissolved in distilled water and to this dimethyl sulfoxide was added. The mixture was stirred for 1 hour, then left to stand for 8 hours. A cream solid was filtered off, washed with distilled water, ethanol and diethyl ether and dried over vacuum. Yield: 380mg (74.8%).

Complex 3: cis-[PtCl₂(DMSO)₂] (15.6mg, 0.04 mmol) was stirred for 24 hours in dichloromethane with complex 2 (20mg, 0.02mmol) in the dark. The yellow solid was washed with dichloromethane and diethyl ether and was dried in vacuo. Yield: 32.4mg (57%). CHN Analysis: C₅₈H₅₀Cl₅N₁₀IrPt₂: Calculated: C: 42.30; H: 3.06; N: 8.51. Found: C: 42.38; H: 3.21; N: 8.85. Exact Mass: 1645.15[M]; [M]+Na⁺ = 1668.1090; {[M]³⁺ -H⁺}/2 = 769.1273; {[M]⁴⁺ -2H⁺}/2 = 751.1355; [M]³⁺/3 = 513.0855.

^1H NMR (400MHz, DMSO-d₆) δ (ppm): 8.93(d, 2H, $J = 9.16$); 8.53(d, 2H, $J = 6.87$); 8.32(t, 2H, $J = 7.63$); 8.17(t, 2H, $J = 7.63$); 8.09(t, 4H, $J = 6.87$); 7.94(t, 2H, $J = 7.63$); 7.84 (t, 2H, $J = 6.87$); 7.68(d, 4H, $J = 8.39$); 7.63-7.59(m, 8H); 7.51(2H, d, $J = 6.87$); 7.30(4H, t, $J = 6.10$); 7.08(2H, d, $J = 5.07$); 6.43(2H, s); 5.44-5.24(8H, m); 5.04-4.86(4H, m).

^{13}C NMR (500MHz, DMSO-d₆) δ (ppm): 166.10, 165.51, 164.82, 155.32, 149.53, 148.74, 148.14, 144.16, 140.92, 139.85, 138.66, 136.05, 132.67, 128.63, 125.87, 125.27, 124.59, 123.37, 121.10, 67.94, 67.82, 67.29, 54.74.

Protein binding and Phosphorescence

Bacterially expressed hexa histidine-tagged protein was partially purified by affinity chromatography using Ni-NTA Agarose (QIAGEN) following manufacture's protocol. For emission studies, His-tagged protein, BSA (Sigma Aldrich), Complex-3, Ni-NTA (Qiagen) and Ni(NO₃)₂ were diluted in lysis buffer (50mM NaH₂PO₄, 300mM NaCl, pH-8) to get the required concentrations. Phosphorescence emission measurements were done at 488 nm excitation and 535 nm emission in Chameleon multilabel detection plate reader (Hidex).

Protein staining

Purified His-tagged protein and BSA at various concentrations were resolved using 10% SDS-polyacrylamide gel electrophoresis followed by staining with complex 3 in 30% methanol for 2 h. Unbound complex 3 was washed with either water or 30% methanol solution. Gels were destained with 30% methanol for either 12 h or 24 h. SYPRO RUBY (Invitrogen) staining was done according to manufacturer's protocol. All the gels were imaged using Typhoon Trio multimode imager (GE Healthcare) at 488 nm excitation wavelength and 535 nm emission wavelength.

Conclusions

Together, the above observations show that fluorescent heterobimetallic Ir(II)/Pt(II) complexes are a new class of protein-binding agents, which can bind to proteins both in solution and in gel with high sensitivity, based on specific interaction with the amino acid histidine. This opens up the possibility of application of such compounds as protein staining agents in both 1D and 2D gel electrophoresis and for cellular staining and imaging. The combination of emissive iridium centre with histidine binding non-emissive platinum centre allows versatile application for efficient staining of histidine-rich proteins. As the fluorescent emission from the Ir(III) centre is dependent on auxiliary ligands, such compounds can potentially be tuned to different wavelengths of excitation and emission without affecting protein binding, thereby enhancing the versatility of applications of such compounds as fluorescent probes and staining agents.

Conflicts of interest

"There are no conflicts to declare".

Acknowledgements

Ankita Sarkar and Bishnu Das is thankful to INSPIRE, New Delhi and IISER Kolkata respectively for their Junior Research Fellowship and Ravi Kumar is thankful to CSIR India for his Senior Research Fellowship. This work is supported by IISER Kolkata and DST-SERB EMR Research Grant EMR/2016/003525 awarded to Partho Sarothi Ray.

Notes and references

- 1 a) V. W. W. Yam and K. M. C. Wong, *Chem. Commun.*, 2011, **47**, 11579 - 11592. b) Y. You, S. Cho and W. Nam, *Inorg. Chem.*, 2014, **53**, 1804-1815. c) L. Flamigni, J. P. Collin, J. P. Sauvage, *Acc. Chem. Res.*, 2008, **41**, 857-871. d) Y. Suzuki, I. Mizuno, Y. Tabei, Y. Fujioka, K. Shinozaki, T. Sugaya and K. Ishihara, *Inorg. Chem.*, 2019, **58**, 9663-9671. e) W. Che, G. Li, X. Liu, K. Shao, D. Zhu, Z. Su, and M. R. Bryce, *Chem. Commun.*, 2018, **54**, 1730-1733. f) D. L. Ma, S. Lin, W. Wang, C. Yang and C. H. Leung, *Chem. Sci.*, 2017, **8**, 878 - 889. g) N. V. Nghia, J. Oh, J. Jung and M. H. Lee, *Organometallics*, 2017, **36**, 2573 - 2580. h) J. Yang, L. Sun, L. Hao, G. G. Yang, Z. G. Zou, Q. Cao, L. N. Jia and Z. W. Mao, *Chem. Commun.*, 2018, **54**, 271- 274. i) S. Carrara, B. Stringer, A. Shokouhi, P. Ramkissoon, J. Agugiaro, D. J. D Wilson, P. J. Barnard and C. F. Hogan, *ACS Appl. Mater. Interfaces.*, 2018, **10**, 37251-37257. j) T. Usuki, H. Uchida, K. Omoto, Y. Yamanoi, A. Yamada, M. Iwamura, K. Nozaki and H. Nishihara, *J. Org. Chem.*, 2019, **84**, 10749-10756. k) Y. You and W. Nam, *Chem. Soc. Rev.*, 2012, **41**, 7061-7084. l) C. Caporale, M. Massi, *Coord. Chem. Rev.*, 2018, **363**, 71-91. m) K. Y. Zhang, T. Zhang, H. Wei, Q. Wu, S. Liu, Q. Zhao, and W. Huang, *Chem. Sci.*, 2018, **9**, 7236-7240. n) K. K. S. Tso, K. K. W. Lo, *Iridium (III) in Optoelectronic and Photonics Applications.*, 2017, **1**, 415-477. o) K. K. W. Lo, *Acc. Chem. Res.*, 2015, **48**, 2985 - 2995. p) Y. Zheng, A. S. Batsanov, M. A. Fox, H. A. A. Attar, K. Abdullah, V. Jankus, M. R. Bryce and P. M. Andrew, *Angew. Chem. Int. Ed.*, 2014, **53**, 11616 - 11619. q) A. Chakraborty, J. E. Yarnell, R. D. Sommer, S. Roy and F. N. Castellano, *Inorg. Chem.*, 2018, **57**, 1298-1310. r) S. Fertes, A. J. Chueca, L. Arnal, A. Martín, U. Giovanella, C. Botta and V. Sicilia, *Inorg. Chem.*, 2017, **56**, 4829-4839. s) O. J. Stacey, A. J. Amoroso, J. A. Platts, P. N. Horton, S. J. Coles, D. Lloyd, C. F. Williams, A. J. Hayes, J. J. Dunsford and S. J. A. Pope, *Chem. Commun.*, 2015, **51**, 12305 - 12308. t) W. A. Tarran, G. R. Freeman, L. Murphy, A. M. Benham, R. Katakay and J. A. Gareth Williams, *Inorg. Chem.*, 2014, **53**, 5738 - 5749. u) N. Cutillas, G. S. Yellol, H. C. de, C. Vicente, V. Rodriguez and J. Ruiz, *Coord. Chem. Rev.*, 2013, **257**, 2784 - 2797.
- 2 a) Y. Zhou, J. Jia, L. Cai and Y. Huang, *Dalton Trans.*, 2018, **4**, 693-699. b) P. Wu, E. L. M. Wong, D. L. Ma, G. S. M. Tong, K. M. Ng and C. M. Che, *Chem. Eur. J.*, 2009, **15**, 3652-3656. c) E. Heinen, *Histochemistry*, 1977, **51**, 257 - 260. d) J. A. Babitch, D. L. Helseth and T. C. Chiu., *Histochemistry*, 1976, **49**, 253-261. e) Y. Zhou, J. Jia, X. Wang, W. Guo, Z. Wu and N. Xu, *Chem. Eur. J.*, 2016, **22**, 16796-16800. f) J. Jia, H. Fei and M. Zhou, *Electrophoresis*, 2012, **33**, 1397-1401. g) D. L. Ma, W. L. Wong, W. H. Chung, F. Y. Chan, P. K. So, T. S. Lai, Z. Y. Zhou, Y. C. Leung and K. Y. Wong, *Angew. Chem.*, 2008, **47**, 3735-3739. h) K. N. Berggren, B. Schulenberg, M. F. Lopez, T. H. Steinberg, A. Bogdanova, G. Smejkal, A. Wang and W. F. Patton, *Proteomics*, 2002, **2**, 486-498. i) K. N. Berggren, T. H. Steinberg, W. M. Lauber, J. A. Carroll, M. F. Lopez, E. Chernokalskaya, L. Zieske, Z. Diwu, R. P. Haugland and W. F. Patton, *Anal. Biochem.*, 1999, **276**, 129-143. j) C. Tokarski, C. Cren-Olive, M. Fillet, C. Rolando and Christian, *Electrophoresis*, 2006, **27**, 1407-1416.
- 3 a) C. L. Ho, K.-L. Wong, H.-K. Kong, Y.-M. Ho, C. T.-L. Chan, W.-M. Kwok, K. S.-Y. Leung, H.-L. Tam, M. H.-W. Lam, X.-F. Ren, A.-M. Ren, J.-K. Feng and W.-Y. Wong, *Chem. Commun.*, 2012, **48**, 2525 - 2527. b) H. Sun, L. Yang, H. Yang, S. Liu, W. Xu, X. Liu, Z. Tu, H. Su, Q. Zhao and W. Huang, *RSC Adv.*, 2013, **3**, 8766 - 8776.
- 4 L. Xiong, Q. Zhao, H. Chen, Y. Wu, Z. Dong, Z. Zhou and F. Li, *Inorg. Chem.*, 2010, **49**, 6402 - 6408.
- 5 a) L. Flamigni, A. Barbieri, C. Sabatini, B. Ventura and F. Barigelletti, *Top. Curr. Chem.*, 2007, **281**, 143. (b) J. A. G. Williams, A. J. Wilkinson and V. L. Whittle, *Dalton Trans.*, 2008, 2081 - 2099.
- 6 M. J. Frisch, G. W. Trucks, H. B. Schlegel, G. E. Scuseria, J. R. Cheeseman, G. Scalmani, et al. 2009 Gaussian 09. B.01 Gaussian, Inc., Wallingford, CT.
- 7 a) K. K.-W. Lo, C.-K. Chung and N. Zhu, *Chem. Eur. J.*, 2003, **9**, 475 - 483. b) C. E. Welby, L. Gilmartin, R. R. Marriott, A. Zahid, C. R. Rice, E. A. Gibson and P. I. P. Elliott, *Dalton Trans.*, 2013, **42**, 13527 - 13536.
- 8 a) A. F. Yang, S. L. Hou, Y. Shi, G. L. Yang, D. B. Qin, and B. Zhao, *Inorg. Chem.*, 2019, **58**, 6356-6362. b) P.

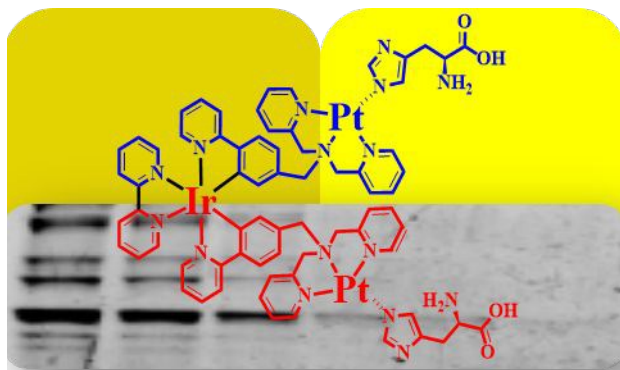
ARTICLE

Journal Name

- Chandrasekhar, A. Mukhopadhyay, G. Savitha and J. N. Moorthy, *Chem. Sci.*, 2016, **7**, 3085-3091. c) H. Ito and S. Shinoda, *Chem. Commun.*, 2015, **51**, 3808-3811. d) J. Wang, H. B. Liua, Z. Tonga and C. S. Hab, *Coord. Chem. Rev.*, 2015, **303**, 139 - 184.
- 9 A. I. Solomatina, P. S. Chelushkin, D. V. Krupenya, I. S. Podkorytov, T. O. Artamonova, V. V. Sizov, A. S. Melnikov, V. V. Gurzhiy, E. I. Koshel, V. I. Shcheslavskiy and S. P. Tunik, *Bioconjugate Chem.*, 2017, **28**, 426 - 437.
- 10 a) N. Yoshinari, T. Shimizu, K. Nozaki and T. Konno, *Inorg. Chem.* 2016, **55**, 2030-2036. b) S. Hadi and T. G. Appleton, *Pol. J. Chem.*, 2009, **83**, 437-443.
- 11 V. Lingen, A. Lüning, A. Krest, G. B. Deacon, J. Schur, I. Ott, I. Pantenburg, G. Meyer and A. Klein, *J. Inorg. Biochem.*, 2016 **165**, 119-127.

View Article Online
DOI: 10.1039/C9DT04720D

TOC Graphic

View Article Online
DOI: 10.1039/C9DT04720D**Cyclometalated Trinuclear Ir(III)/Pt(II) Complex as a Luminescent probe for Histidine-rich Proteins**Ankita Sarkar,^{a‡} Ravi Kumar,^{b‡} Bishnu Das,^a Partho Sarothi Ray,^{*b} Parna Gupta^{*a}

A trinuclear luminescent organometallic Pt-Ir-Pt complex acts as efficient protein staining agent due to reversible binding to histidine-rich proteins.